Male germ cells and photoreceptors, both dependent on close cell–cell interactions, degenerate upon ClC-2 Cl⁻ channel disruption

Michael R.Bösl[1], Valentin Stein[1], Christian Hübner[1], Anselm A.Zdebik[1], Sven-Eric Jordt[1,2], Amal K.Mukhopadhyay[3], Michail S.Davidoff[4], Adolf-Friedrich Holstein[4] and Thomas J.Jentsch[1,5]

[1]Zentrum für Molekulare Neurobiologie Hamburg (ZMNH), [4]Institut für Anatomie, Universität Hamburg, Martinistraße 52, D-20246 Hamburg and [3]Institut für Hormon- und Fortpflanzungsforschung (IHF), Grandweg 64, D-22529 Hamburg, Germany

[2]Present address: Department of Cellular and Molecular Pharmacology, University of California at San Francisco, 513 Parnassus Avenue, San Francisco, CA 94143-0450, USA

[5]Corresponding author
e-mail: jentsch@zmnh.uni-hamburg.de

M.R.Bösl and V.Stein contributed equally to this work

The functions of some CLC Cl⁻ channels are evident from human diseases that result from their mutations, but the role of the broadly expressed ClC-2 Cl⁻ channel is less clear. Several important functions have been attributed to ClC-2, but contrary to these expectations ClC-2-deficient mice lacked overt abnormalities except for a severe degeneration of the retina and the testes, which led to selective male infertility. Seminiferous tubules did not develop lumina and germ cells failed to complete meiosis. Beginning around puberty there was a massive death of primary spermatocytes and later also of spermatogonia. Tubules were filled with abnormal Sertoli cells, which normally express ClC-2 in patches adjacent to germ cells. In the retina, photoreceptors lacked normal outer segments and degenerated between days P10 and P30. The current across the retinal pigment epithelium was severely reduced at P36. Thus, ClC-2 disruption entails the death of two cell types which depend on supporting cells that form the blood–testes and blood–retina barriers. We propose that ClC-2 is crucial for controlling the ionic environment of these cells.
Keywords: anion channel/epilepsy/knock-out/retinal degeneration/Sertoli cell only syndrome

Introduction

The Cl⁻ channel ClC-2 (Thiemann *et al.*, 1992) belongs to the gene family of CLC channels that includes nine different members in mammals and was highly conserved in evolution (for review see Jentsch *et al.*, 1999). Based on homology, these channels can be grouped into three different classes. Channels of the first class (which includes ClC-2) are plasma membrane Cl⁻ channels, whereas members of the two other classes probably perform their function mainly in intracellular membranes.

The physiological importance of some of these channels is revealed by diseases that result from mutations in their genes. Thus, mutations in ClC-1 lead to myotonia (Koch *et al.*, 1992), a disease associated with electrical hyperexcitability of the muscle membrane. Mutations in the renal channel ClC-Kb cause a form of Bartter's syndrome, a disease associated with a massive salt loss (Simon *et al.*, 1997), and the disruption of ClC-K1 in mice leads to diabetes insipidus (Matsumura *et al.*, 1999). Both phenotypes indicate that these channels are present in the plasma membrane and function in transepithelial transport.

By contrast, ClC-5 is expressed in endosomes and probably contributes to their acidification (Günther *et al.*, 1998). Its disruption in Dent's disease leads to proteinuria and kidney stones (Lloyd *et al.*, 1996). Both symptoms result from a defect in proximal tubular endocytosis that secondarily changes levels of calciotropic hormones (Piwon *et al.*, 2000). ClC-3, a close homolog of ClC-5, is also present in endosomal compartments and contributes to the acidification of synaptic vesicles (Stobrawa *et al.*, 2001). Its disruption in mice leads to a degenerative loss of the hippocampus and photoreceptors. Finally, mutational inactivation of the ClC-7 Cl⁻ channel leads to severe osteopetrosis in mice and man (Kornak *et al.*, 2001). This broadly expressed channel is present in late endosomal and lysosomal compartments and is inserted together with the proton pump into the ruffled border of osteoclasts (Kornak *et al.*, 2001).

The function of other CLC channels is less clear. ClC-2 is almost ubiquitously expressed (Thiemann *et al.*, 1992). It is largely closed under resting conditions, but activates slowly upon hyperpolarization (Thiemann *et al.*, 1992). It is also activated by acidic extracellular pH (Jordt and Jentsch, 1997) and by osmotic cell swelling (Gründer *et al.*, 1992). The latter finding suggested a role in cell volume regulation (Gründer *et al.*, 1992; Furukawa *et al.*, 1998; Xiong *et al.*, 1999). However, most studies of swelling-activated currents in native tissues have revealed the presence of an anion channel that differs in its biophysical characteristics, and may dominate the response to swelling (Worrell *et al.*, 1989; Solc and Wine, 1991; Jackson and Strange, 1995; Strange *et al.*, 1996).

Several other functions were suggested for ClC-2. Its apical expression in fetal lung epithelia led to the proposal that it is essential for lung development (Murray *et al.*, 1995; Blaisdell *et al.*, 2000). This localization also suggested that ClC-2 might be an alternative pathway for Cl⁻ secretion in cystic fibrosis, a potentially lethal disease that is caused by loss-of-function mutations of the cystic fibrosis transmembrane conductance regulator (CFTR) Cl⁻ channel (Thiemann *et al.*, 1992; Schwiebert *et al.*, 1998).

ClC-2 was also postulated to have a key role in early nephrogenesis (Huber et al., 1998), and was assumed to be crucial for gastric acid secretion by providing a Cl⁻ conductance in parallel to the H⁺,K⁺-ATPase (Malinowska et al., 1995). Moreover, ClC-2 may modulate the post-synaptic responses to γ-aminobutyric acid (GABA) and glycine by influencing the intracellular Cl⁻ concentration in neurons (Smith et al., 1995; Staley et al., 1996).

To test these hypotheses and to elucidate the role of ClC-2 in development and organ physiology, we now disrupted the mouse Clcn2 gene by homologous recombination. In contrast to the speculations mentioned above, we did not find abnormalities in lung or kidney development, nor in gastric acid secretion. We also did not observe seizures that might be expected from a widespread change of responses to GABA from inhibition to excitation. Unexpectedly, we found degenerative changes in the testes and the retina, tissues in which germ cells and photoreceptors, respectively, are in close contact with supporting epithelial cells. The degeneration started when these supporting cells (Sertoli cells and retinal pigment epithelial cells) began to form the blood–testis and blood–retina barrier, respectively. Furthermore, currents across the retinal pigment epithelium (RPE) were severely reduced in Clcn2⁻/⁻ mice. Thus, ClC-2 may play a crucial role in the interaction between these cells, probably by controlling their ionic environment.

Results

Generation of Clcn2-deficient mice

We disrupted the Clcn2 locus in mice by homologous recombination using a replacement vector with positive (neo) and negative (dta) selection markers (Figure 1A). This deleted the genomic sequence encoding transmembrane segments D2–D6, which are important for ion permeation (Steinmeyer et al., 1994; Ludewig et al., 1996; Fahlke et al., 1997), and also severely truncated the protein. Recombinant embryonic stem (ES) cells were screened by genomic Southern blotting (Figure 1B). The generation of a true null mutant was confirmed by northern and western blotting. In homozygous ClC-2 knock-out mice (Clcn2⁻/⁻), the normal ~3.4 kb ClC-2 mRNA was replaced by a truncated 2.2 kb transcript consisting of the 5′ part of ClC-2 fused to the Neo gene (Figure 1C). Identical hybridization signals were obtained with a ClC-2 5′-probe and with a Neo-probe, but no signal was obtained with a ClC-2 3′-probe. In western blots, an antibody directed against the C-terminus of ClC-2 recognized bands of the appropriate size in lysates of various tissues of wild-type (WT), but not of Clcn2⁻/⁻ animals (Figure 1D and data not shown).

Clcn2⁻/⁻ mice were viable, grew normally, and showed no immediately visible physical or behavioral abnormalities. Although ClC-2 was suggested to be important for lung (Murray et al., 1995) and kidney (Huber et al., 1998) development, there were no gross anatomical or histological changes in these tissues (not shown). Also, histological analysis of the liver and the pancreas did not reveal abnormalities (not shown). Serum electrolyte concentrations (Na⁺, K⁺, Ca²⁺, Cl⁻), serum creatinine and serum concentrations of liver-derived enzymes (glutamate oxaloacetate transaminase, glutamate dehydrogenase)
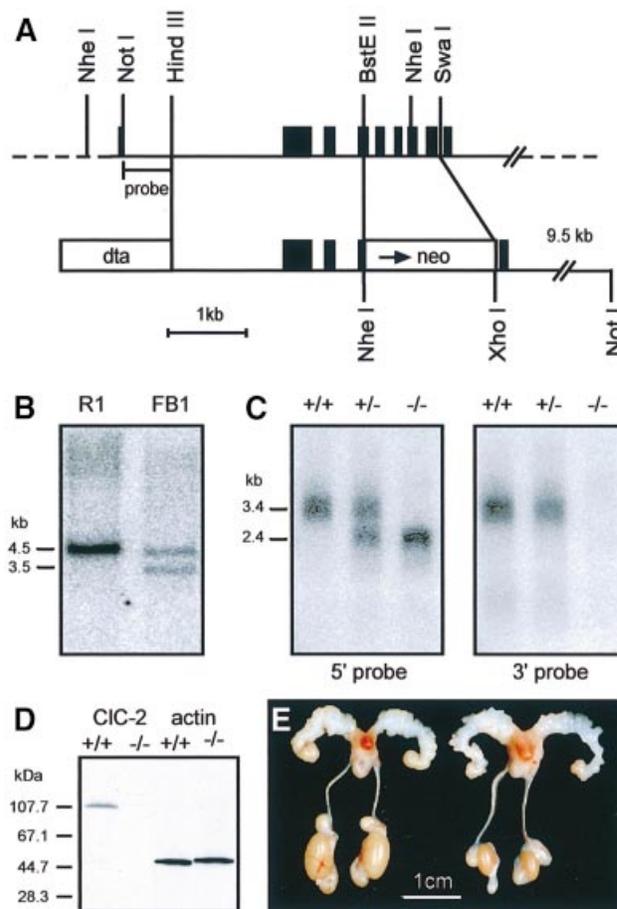

Fig. 1. Generation of ClC-2 knock-out mice. (**A**) Targeting construct. The sequence between the BstEII and SwaI restriction sites of a genomic clone (top) was replaced by a neomycin resistance cassette (bottom). This deletes exons 3–7 totally or partially (exons are shown in black). A diphtheria toxin α gene (dta) was used to select against random integration. (**B**) Southern analysis of genomic DNA from parental ES cells (left) and a correctly targeted ES cell clone (Clcn2⁺/⁻) (right). The DNA was restricted with NheI, and the blot was probed with the NotI–HindIII fragment shown in (A). Correctly targeted cells have an additional shorter NheI fragment. (**C**) Northern analysis of testes mRNA from +/+, +/– and –/– mice using a 5′ (left) and a 3′ (right) ClC-2 probe. (**D**) Immunoblot of testes protein lysate from +/+ and –/– mice using an antibody directed against the ClC-2 C-terminus. It detects a protein of the correct size (~100 kDa) in +/+, but not in –/– mice. An antibody against actin was used as a loading control. (**E**) Macroscopic male reproductive tract phenotype. Testes of adult Clcn2⁻/⁻ mice (right) are smaller than those of +/+ males (left). Epididymis and seminal vesicles are of the same size. Testes from +/– animals were not different from those of +/+ mice (not shown).

were also in the normal range. ClC-2 was also proposed to be essential for acid secretion in the stomach (Malinowska et al., 1995), but there was no significant difference in gastric acidification. Treatment with histamine decreased gastric pH from 3.8 ± 0.4 to 2.3 ± 0.3 in WT mice (n = 5), and from 4.0 ± 0.3 to 2.5 ± 0.3 in Clcn2⁻/⁻ mice (n = 5).

ClC-2 is also thought to regulate neuronal intracellular Cl⁻ concentration, thereby influencing the response to the neurotransmitter GABA (Smith et al., 1995; Staley et al., 1996). However, Clcn2⁻/⁻ animals showed no overt seizures that may result from excitatory effects of GABA or glycine, nor did we observe an increased

sensitivity to flurothyl, which was used to induce seizures (Prichard *et al.*, 1969) (data not shown).

Testicular degeneration in Clcn2⁻/⁻ mice

Despite normal copulatory behavior and vaginal plug formation in female mice, *Clcn2⁻/⁻* males did not produce offspring. Heterozygous *Clcn2⁺/⁻* males and *Clcn2⁻/⁻* females were fertile. At autopsy, the gross anatomy of male –/– mice appeared normal except for a testes pathology. Testes of adult –/– mice were markedly reduced in size (Figure 1E). This size difference gradually became apparent after 3 weeks, the onset of puberty in mice. The size of the epididymis and seminal vesicles appeared unchanged. Dissection of the epididymis of WT or +/– mice showed massive amounts of mature sperms, which were totally absent in –/– animals.

Histological examination of adult –/– testes revealed degenerated seminiferous tubules with markedly reduced diameters and missing lumina. The obliterated lumina were filled with numerous membranous extensions of abnormal Sertoli cells (Figure 2Be). Germ cells of any stage were lacking in –/– males older than 6 months and spermatids could never be detected. The relative number of interstitial Leydig cells was increased (Figure 2Ca and Da). In contrast, tubules of age-matched +/+ or +/– littermates had open lumina and displayed normal spermatogenesis with the full spectrum of spermatogonia, spermatocytes and spermatids at various stages of development (Figure 2Ae).

The time course of the testicular changes was followed during post-natal development (Figure 2). There was no apparent difference in testes histology in the first week after birth (Figure 2Aa and Ba). At 2 weeks, the germinal epithelium of –/– mice already appeared disorganized (Figure 2Ab and Bb). Spermatogonia and primary spermatocytes were still detectable in both genotypes. Some tubules of +/+ animals already had small lumina. At 3 weeks, most +/+ seminiferous tubules had a lumen, were expanded at least 2-fold in diameter, and contained large numbers of spermatogonia and spermatocytes (Figure 2Ac). By contrast, –/– tubules lacked lumina and contained predominantly Sertoli cells, a few spermatogonia and abnormal clusters of primary spermatocytes (Figure 2Bc). Electron microscopy revealed that the cells within these clumps were connected by apparently normal cytoplasmic bridges (data not shown). The chromosomes of some spermatocytes showed synaptonemal complexes, indicating that these cells had entered the prophase of meiosis. By week 4, the diameter of WT and +/– tubules had increased to ~170 μm, and most tubules exhibited characteristic waves of differentiating germ cells including large numbers of round spermatids (Figure 2Ad). Tubules of –/– animals were much smaller (~110 μm), lacked lumina, and were filled predominantly by Sertoli cells (Figure 2Bd). Their protrusions did not yet show the parallel alignment as observed in –/– adults. There were still some residual spermatogonia at the base and a few clumps of degenerating primary spermatocytes in the adluminal compartment. Post-meiotic spermatids were missing completely.

We also followed the fate of the germ cells by using an antibody against the germ-cell-specific nuclear antigen GCNA1 (Enders and May, 1994). It is expressed in spermatogonia and early spermatocytes, and progressively decreases with further germ cell differentiation. Normal numbers and distributions of germ cells were present in –/– males at 2 weeks (Figure 2Cb and Db). At 3 weeks, GCNA1-positive germ cells were disorganized in –/– tubules (Figure 2Dc) compared with heterozygous (or WT) animals (Figure 2Cc). Only occasional germ cells were present in –/– tubules at 4 weeks (Figure 2Dd). They were completely lost at later stages (Figure 2De).

Immunocytochemistry revealed that ClC-2 was expressed in membranes of Sertoli cells (Figure 3A, C and D). Staining was specific as it was absent in –/– animals (Figure 3B). Staining of Sertoli cell membranes was in patches and was more prominent in the basal third of the germinal epithelium. Staining often occurred at zones contacting germ cells, both spermatogonia and early spermatocytes.

Cl⁻ currents resembling ClC-2 (Gründer *et al.*, 1992; Thiemann *et al.*, 1992) were indeed present in purified Sertoli cells from +/+ animals (Figure 4A), but were missing in –/– Sertoli cells (Figure 4B). These currents showed the typical activation by hyperpolarization. Their Cl⁻ > Br⁻ > I⁻ conductance sequence (data not shown) was identical to that observed with ClC-2 in heterologous expression systems.

Markers of testes development

The expression of markers of germ cell development was examined by northern analysis (Figure 5). Proacrosin binding protein (Nantel *et al.*, 1996) and the germ-cell-specific cyclin Ccna1 (Sweeney *et al.*, 1996) are already expressed in pachytene spermatocytes. Both markers appeared at 3 weeks in +/– mice and were not detected in –/– mice at any age. Prm1, the gene encoding protamine 1, is transcribed in post-meiotic round spermatids (Lee *et al.*, 1995). Prm1 expression began at 3 weeks in +/– mice and increased further after 4 and 6 weeks. Protamine was not observed at any age in –/– mice. Thus, consistent with the histological data, germ cells in ClC-2⁻/⁻ mice do not pass beyond meiosis I.

Sex hormone levels

We determined serum concentrations of testosterone, progesterone, follicle-stimulating hormone (FSH) and luteinizing hormone (LH) in 8-week-old males (Table I). There was no significant difference between animals of different genotypes. The normal size of *Clcn2⁻/⁻* epididymis and seminal vesicles in –/– animals (Figure 1E) also suggests that circulating androgen levels are within the normal range. However, local concentrations of testosterone may not be tightly correlated with serum levels.

LH-induced testosterone secretion by Leydig cells is affected by anion replacement and Cl⁻ channel inhibitors (Choi and Cooke, 1990). It was suggested that a hyperpolarization-activated Cl⁻ current participates in the signal transduction leading to testosterone secretion of Leydig cells (Noulin and Joffre, 1993; Noulin *et al.*, 1996). Although Leydig cells did not stain for ClC-2 in immunocytochemistry (Figure 3) (probably due to the low sensitivity of the antibody and a uniform ClC-2 expression), patch–clamp measurements revealed the
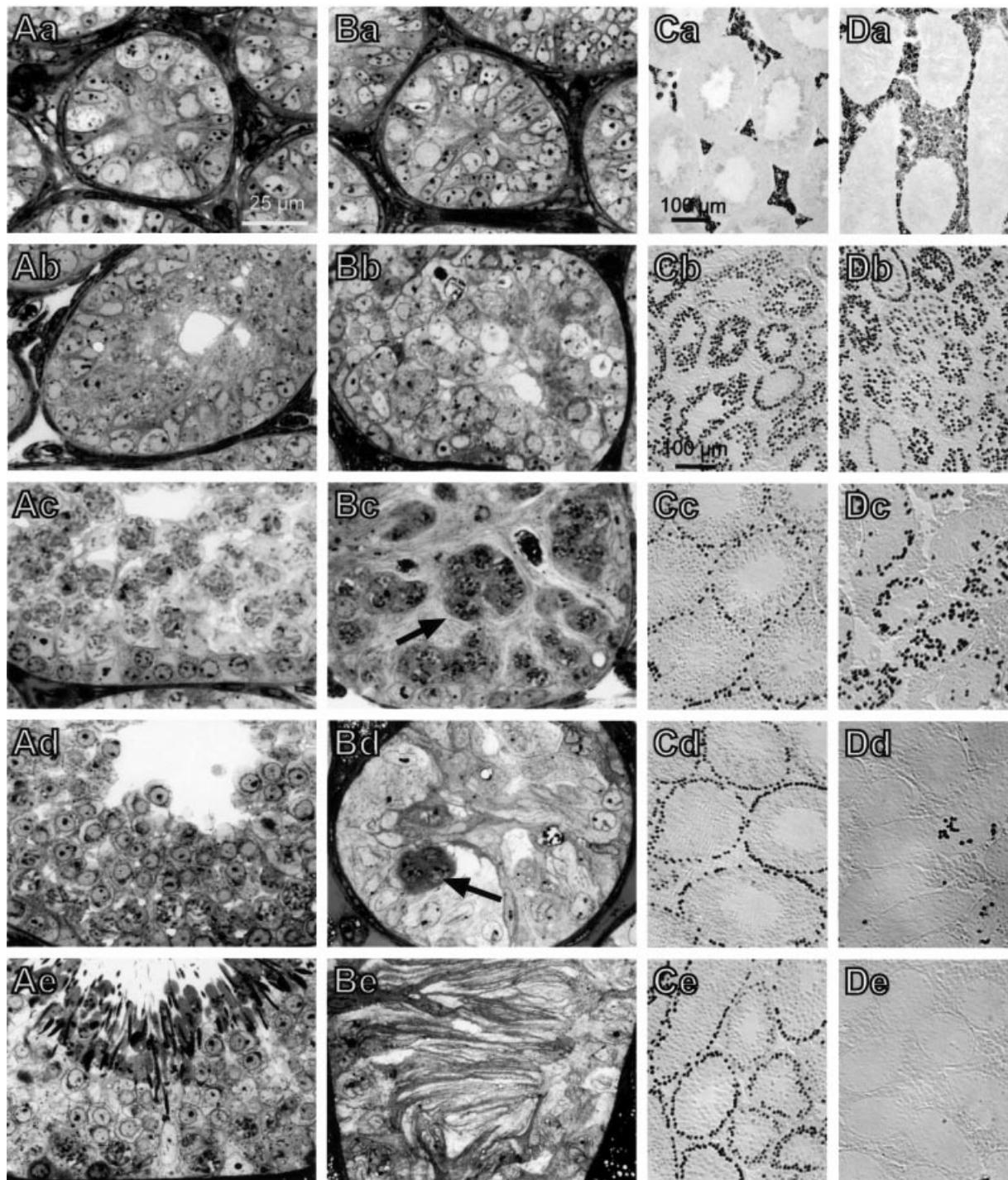
Fig. 2. Histological analysis of post-natal testes development. Semi-thin sections of testes from WT animals (**A**) and ClC-2$^{-/-}$ mice (**B**) obtained 1 (a), 2 (b), 3 (c), 4 (d) and 10 weeks (e) after birth. At 2 weeks, the germinal epithelium is already disorganized in –/– mice (Bb). The normal development leading to a fully developed spermatogenesis in +/+ animals at 10 weeks (Ae) is thwarted in –/– animals. Clusters of dying spermatocytes are present at 3 and 4 weeks (Bc and Bd, arrows) and gradually disappear until the tubule is filled exclusively with abnormal Sertoli cells with long cytoplasmic extrusions. (Ca and Da) Testes sections of *Clcn2* +/+ (Ca) and –/– (Da) mice (12 weeks of age) were stained for cytochrome P450, which is indicative for Leydig cells. This reveals a relative Leydig cell hyperplasia in adult knock-out mice. (Cb–Ce and Db–De) Germ cells stained by the GCNA1 antibody (Enders and May, 1994) in *Clcn2*$^{+/-}$ (**C**) and *Clcn2*$^{-/-}$ (**D**) animals at 2 (b), 3 (c), 4 (d) and 6 weeks (e) of age. Germ cells are gradually lost after 3 weeks of age, with only occasional GCNA1-positive cells being detected at 6 weeks (De). After 3 months, no GCNA1-positive cells could be detected (not shown).

presence of a prominent ClC-2 current (Figure 4C). An inwardly rectifying Cl$^-$ current with the typical activation by hyperpolarization was present in purified Leydig cells isolated from WT but not from –/– animals (Figure 4D). However, in contrast to the hypothesis that this current is

important for testosterone secretion (Choi and Cooke, 1990; Noulin and Joffre, 1993; Noulin *et al.*, 1996), the addition of human chorionic gonadotropin (hCG) or 8-bromo-cAMP to isolated Leydig cells revealed no significant difference in testosterone secretion between
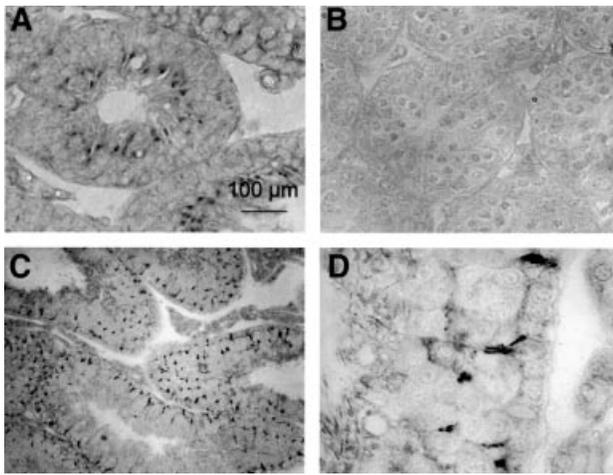
Fig. 3. Immunolocalization of ClC-2 in the testes. (**A**) Histochemical staining for ClC-2 in WT mice and (**B**) ClC-2⁻/⁻ mice at 2 weeks after birth. (**C** and **D**) ClC-2 staining in 10-week-old WT animals; (D) was obtained at a higher magnification. ClC-2 is expressed in Sertoli cell membranes mainly in the basal third of the seminiferous tubule, also adjacent to spermatogonia that are at the *cis* side of the blood–testis barrier (D). *Clcn2⁻/⁻* testes lack immunoreactivity.
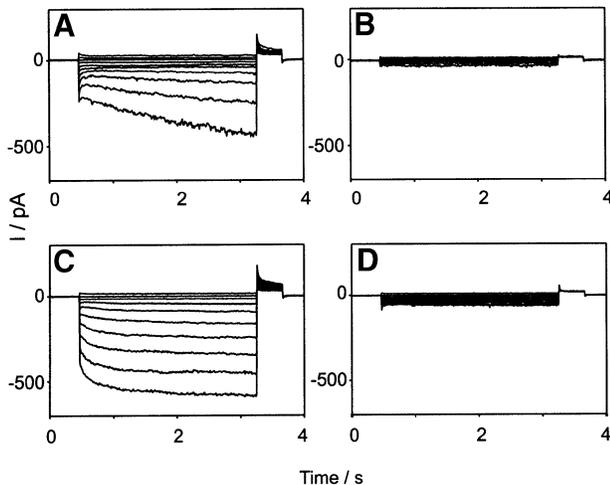

Fig. 4. Inwardly rectifying Cl⁻ currents in Leydig and Sertoli cells are mediated by ClC-2. Whole-cell patch–clamp measurements were performed on purified Sertoli (**A** and **B**) or Leydig (**C** and **D**) cells from +/+ (A and C) or –/– (B and D) animals. Membrane voltages were clamped from +40 to –140 mV in steps of 20 mV. The hyperpolarization-activated Cl⁻ current typical for ClC-2 is missing in cells from –/– animals. Similar currents were obtained from >15 cells of each cell type. The kinetics of ClC-2 currents is variable, and the difference between currents in (A) and (C) is not significant.

Clcn2 genotypes (not shown). Thus, the present testes pathology can not be explained by this hypothesis.

Progressive retinal degeneration in Clcn2⁻/⁻ mice

Behavioral tests revealed that mice lacking ClC-2 were blind. Histological analysis of the retina (Figure 6) showed a dramatic and early loss of photoreceptor cells in *Clcn2⁻/⁻* mice. At P10 (Figure 6A), the outer nuclear layer (ONL), which contains the nuclei and cell bodies of photoreceptors, was indistinguishable from that of control mice (not shown). At P14, however, there was a large number of dark, pyknotic nuclei, and the number of cells in the ONL
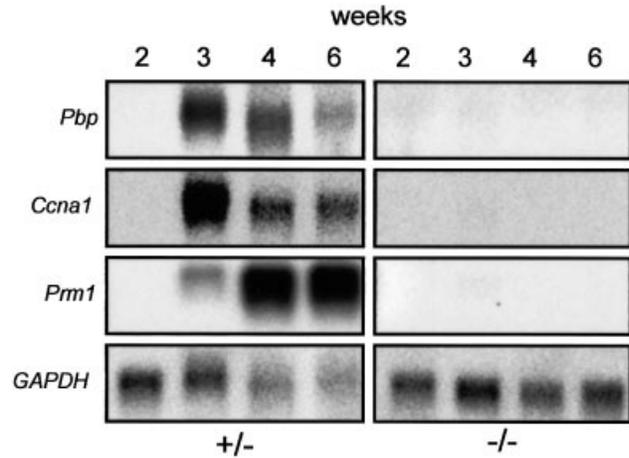

Fig. 5. Expression of germ cell markers in *Clcn2⁺/⁻* and *Clcn2⁻/⁻* mice during development. Northern analysis of testes RNA (~10 μg total RNA per lane) using probes for RNAs encoding proacrosin binding protein (Pbp), a germ-cell-specific cyclin (Ccna1) and protamine 1 (Prm1). Total testes RNA from *Clcn2⁺/⁻* (left) and *Clcn2⁻/⁻* mice (right) at weeks 2, 3, 4 and 6 after birth was analyzed. The loading control GAPDH indicates that less RNA has been loaded for 4- and 6-week-old +/– animals, in part explaining the lower signals in these lanes. None of these markers is detected in –/– animals.

Table I. Determination of serum hormone levels

Hormone	+/+	+/–	–/–
Testosterone male	6.9 ± 2.3	4.2 ± 1.8	3.1 ± 3.5
Progesterone male	4.8 ± 1.2	1.7 ± 0.5	2.9 ± 0.7
FSH male	66.5 ± 7.7 (9)	63.7 ± 5.1 (14)	82.1 ± 6.3 (19)
LH male	1.1 ± 0.6 (9)	1.4 ± 0.3 (14)	0.8 ± 0.2 (19)
Testosterone female	<0.1	0.1 ± 0.1	0.1 ± 0.1

Determination of serum hormone levels (in μg/l) showed no significant difference between genotypes. Testosterone and progesterone were determined in 10 animals; the numbers of animals for LH and FSH are given in parentheses; error = SEM. Testosterone in females was measured as a control.

had decreased by ~50% (Figure 6B). The thickness of the ONL decreased further during the next few weeks, and at P31 only one or two rows of photoreceptor nuclei were present (Figure 6C and D). At P65, only some scattered nuclei remained (Figure 6E). Retinas of heterozygous animals did not differ from WT at any time point (data not shown).

At P10, the outer segments of the photoreceptors of –/– retina were already less developed than in WT (Figure 6F and G). Furthermore, some displaced photoreceptor cells were observed beneath the RPE. Electron micrographs revealed a disorganization of both inner and outer segments at P10. Whereas +/– retinas had parallel lines of outer segments that contained regular stacks of disks (Figure 6J), –/– mice had shortened and whirled outer segments (Figure 6K). At P18 (Figure 6H and I), –/– photoreceptor cells were totally devoid of outer segments. To test whether retinal degeneration could be modulated by exposure to light, we kept mice in the dark from P0 to P35. However, we could not detect any effect on the extent or progress of the retinal degeneration.

Because the present antibody was not suited for retinal immunocytochemistry, we used *in situ* hybridization and
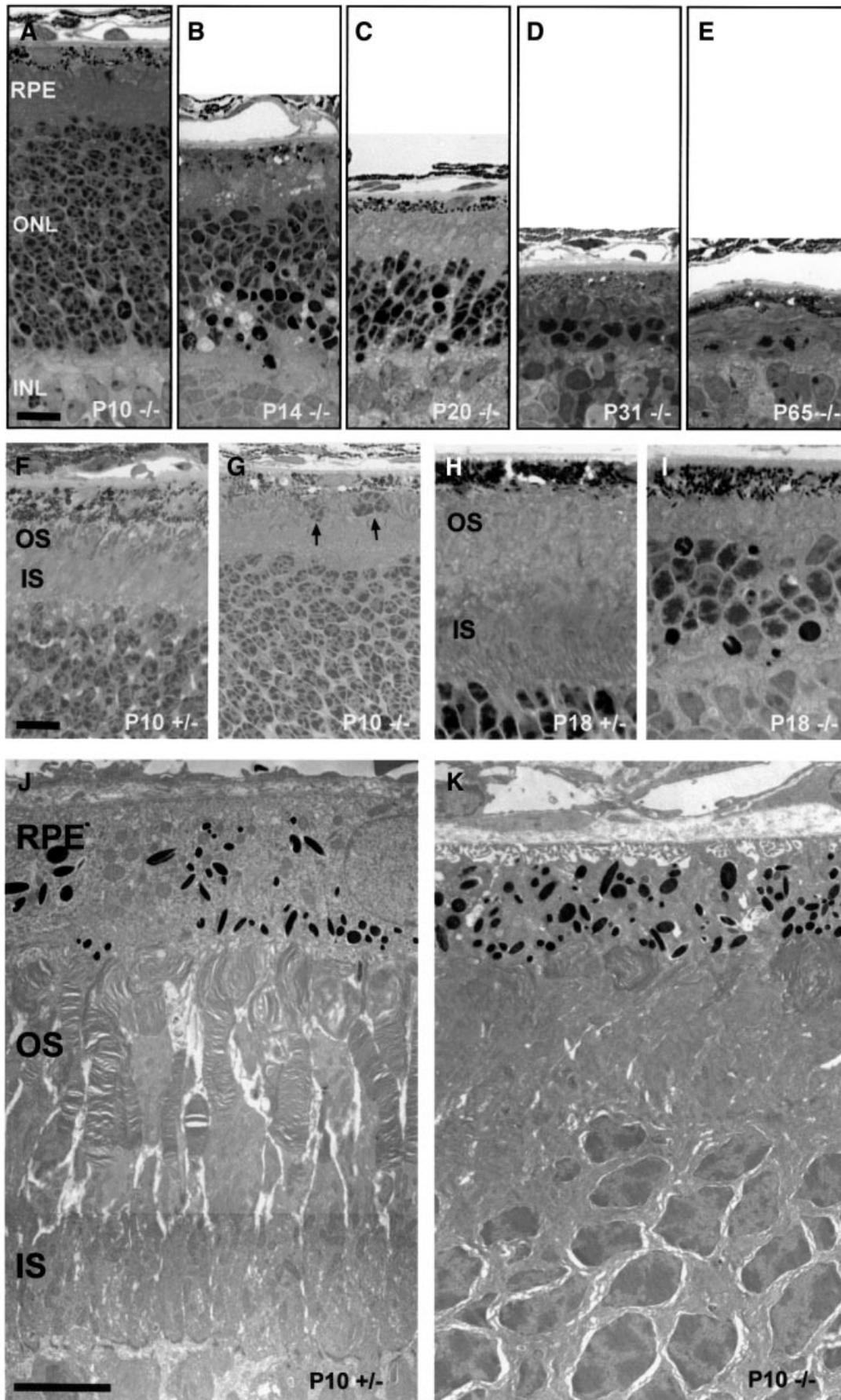
western blotting to determine the expression pattern of ClC-2 (Figure 7). The ClC-2 transcript was detected in the RPE, the inner nuclear layer and the ganglion cell layer, but was less prominent in the ONL, which comprises the nuclei of the photoreceptors (Figure 7B). Western analysis demonstrated the presence of the ClC-2 protein in the neuroretina and in the RPE (Figure 7C).

The photoreceptor degeneration could be due to a cell-intrinsic effect of *Clcn2* disruption. It might also be due to a defect in the RPE that regulates the ionic environment of photoreceptors and provides and removes important metabolites. We therefore assessed the transepithelial transport across the RPE of P36 animals by Ussing chamber experiments (Figure 7D). The transepithelial voltages of RPE preparations from +/– animals were ~6 mV (retina positive), while those from –/– littermates were <0.5 mV. Even though the transepithelial resistance was also reduced, the equivalent short circuit current across the –/– RPE was significantly lower as well. This suggests a defect in active transepithelial transport, which under these experimental conditions reflects mainly Cl⁻ transport (la Cour *et al.*, 1986). We also compared these parameters in +/+ and +/– adult mice. There was no significant difference (data not shown).

Discussion

The functional consequences of disrupting ubiquitously expressed genes are difficult to predict. Even though the respective gene product, in the present case a plasma membrane Cl⁻ channel, may play a physiological role in many tissues, an overt phenotype may be restricted to a limited number of tissues where it plays a role that can not be compensated by other proteins. Unexpectedly, we found that the loss of ClC-2 entailed a degeneration of the testes and the retina. The close spatial and functional relationship between Sertoli cells and germ cells, or retinal pigment epithelial cells and photoreceptors, respectively, suggests that the function of ClC-2 may be important for their interactions. Interestingly, the severe and ultimately complete degeneration of germ cells and photoreceptors began at a time when the blood–organ barrier is established in these organs. The altered morphology of Sertoli cells and the defect in RPE transport suggest that ClC-2 has its most crucial role in these nursing cells.

Several previous hypotheses on the physiological functions of ClC-2 are not supported by the mouse model

Based on its biophysical properties and spatial as well as temporal expression patterns, several functions were assigned to ClC-2. It is expressed in apical membranes of lung epithelia, where it may play a role in Cl⁻ and fluid

secretion similar to the cAMP-activated Cl⁻ channel CFTR (Murray *et al.*, 1995; Schwiebert *et al.*, 1998; Blaisdell *et al.*, 2000). ClC-2, but not CFTR, is expressed in fetal lung. Because lung development is known to depend on fluid secretion, ClC-2 was postulated to be important for the development of the lung (Murray *et al.*, 1995; Blaisdell *et al.*, 2000). While the present knock-out does not support this notion, it does not rule out the possibility that ClC-2 participates in pulmonary transepithelial Cl⁻ transport. That ClC-2, in principle, may play a role in transepithelial
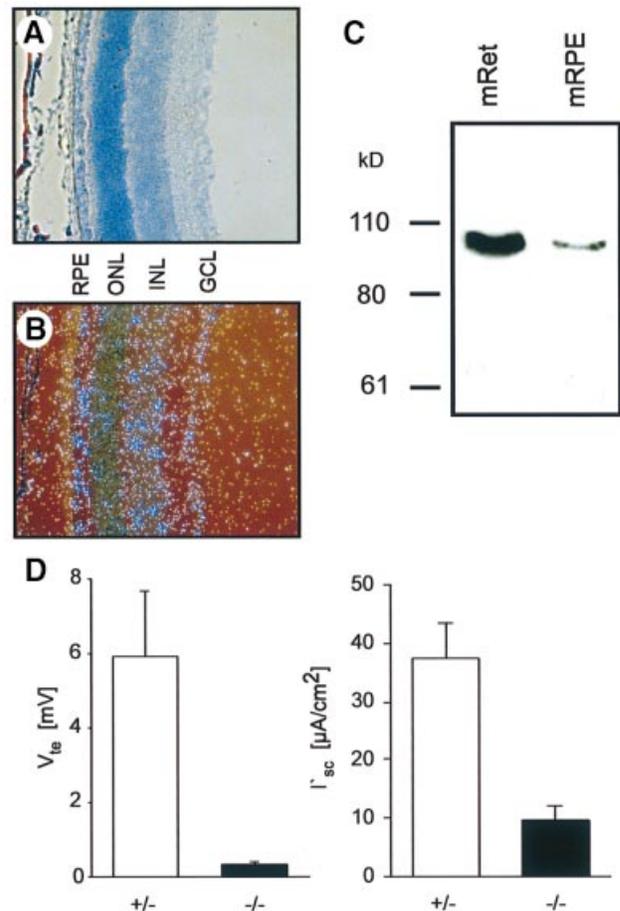

Fig. 7. Localization and function of ClC-2 in the retina and the RPE. (A–C) Expression of ClC-2 in the retina by *in situ* hybridization (**B**) and western blotting (**C**). Membranes from mouse retina (mRet) and mouse RPE (mRPE) were analyzed. (**A**) A Giemsa-stained retinal section. In (**B**), the ClC-2 transcript was detected in the RPE, the inner nuclear layer (INL) and the ganglia cell layer (GCL). The staining of the ONL, which comprises the nuclei of photoreceptors, was somewhat weaker. (**D**) Results from Ussing chamber experiments of P36 RPE preparations. The transepithelial voltage, V_{te}, and the equivalent short circuit current I'_{sc} are significantly reduced in *Clcn2*⁻/⁻ animals ($n = 5$) compared with +/– animals ($n = 10$); error bars indicate SEM.

Fig. 6. Retinal degeneration in *Clcn2*⁻/⁻ mice. Retinal sections of *Clcn2*⁻/⁻ mice at lower magnification show the temporal pattern of the rapid loss of photoreceptor cells (A–E) between post-natal day P10 (**A**), P14 (**B**), P20 (**C**), P31 (**D**) and P65 (**E**). At P10, the thickness and cell number in the ONL did not differ from heterozygous animals or WT controls (not shown). A detailed view at higher magnification demonstrates the development of the inner (IS) and outer segment (OS) between P10 (**F**) and P18 (**H**) in heterozygous animals compared with *Clcn2*⁻/⁻ mutant mice (**G** and **I**). In *Clcn2*⁻/⁻ mice the OS is less developed at P10 (G) and completely absent at P18 (I), when the IS is also reduced in length. Arrows in (G) hint at dislocated photoreceptor cells beneath the RPE in *Clcn2*⁻/⁻ mice. Electron micrographs of this retinal zone at P10 (**J** and **K**). In *Clcn2*⁻/⁻ mice, the IS and OS are disorganized, the outer segments are compacted, extremely shortened and whirled (K), whereas in heterozygous controls (J) they protrude and elongate towards the RPE in regularly stacked discs. INL, inner nuclear layer. Scale bars: (A–E), 20 μm; (F–I), 10 μm; (J and K), 5 μm.

transport is supported by our Ussing chamber experiments on RPE preparations. Future studies using mice disrupted for both ClC-2 and CFTR should be able to address this medically important question.

Two other hypotheses concerning the function of ClC-2 were also invalidated by the present mouse model. The normal kidney development of *Clcn2−/−* mice shows that ClC-2 is not needed in this process (Huber *et al.*, 1998), and the normal gastric acidification disproves the previous notion that it is rate-limiting for proton secretion in the stomach (Malinowska *et al.*, 1995).

The question of whether ClC-2 participates in regulating the intracellular Cl− concentration in neurons may be more complex. The electrochemical potential for Cl− determines whether $GABA_A$− or glycine-receptor Cl− channels are inhibitory or excitatory. The latter situation occurs in fetal and early post-natal life and is deemed to be important for the development of the nervous system (Cherubini *et al.*, 1991). The expression of ClC-2, which is partially open at resting membrane potentials, may prevent a rise of intracellular Cl− above equilibrium, thus ensuring an inhibitory response. Staley and colleagues (Staley, 1994; Smith *et al.*, 1995) have correlated the expression of ClC-2 and the associated inward currents with an inhibitory response to GABA. Furthermore, heterologous expression of ClC-2 in dorsal root ganglia converted their response to GABA from excitatory to inhibitory (Staley *et al.*, 1996). An extensive excitatory GABA response, as might be expected with a loss of ClC-2 function, may lead to seizures. Intriguingly, a genome search for susceptibility loci of common idiopathic generalized epilepsy identified a locus at 3q26 (Sander *et al.*, 2000) in the vicinity of the human *CLCN2* gene (Protopopov *et al.*, 1996). However, no spontaneous seizures were observed in *Clcn2−/−* mice, and the threshold to a seizure-inducing agent was not changed significantly. This seems to rule out a widespread, dominant role of ClC-2 in the regulation of neuronal intracellular Cl−. Several cation–Cl− cotransporters, including the neuronal K+Cl− cotransporter KCC2, which lowers the intracellular Cl− concentration below electrochemical equilibrium, may play a more prominent role (Rivera *et al.*, 1999). However, we certainly can not exclude a more subtle influence of ClC-2 on neuronal function, as our assays are investigating only gross effects.

ClC-2 is important for cells that depend on epithelia forming blood–organ barriers

The disruption of ClC-2 had a dramatic impact on two organs whose interior is protected by a blood–organ barrier: the seminiferous tubule of the testis and the retina. In both tissues, the cells that depend on the barrier-forming epithelium degenerate.

In the testes, tight junctions between Sertoli cells effectively isolate the (ad)luminal compartment of seminiferous tubules. Germ stem cells and spermatogonia are located on the *cis* (blood) side of the barrier and, after mitosis, migrate through clefts between Sertoli cells into the adluminal compartment in which meiosis and the differentiation to sperm take place. Mature sperms are eventually released into the lumen, which contains a potassium-rich fluid that is secreted by Sertoli cells. The differentiation to sperm cells requires a tight physical association with Sertoli cells. These latter cells not only

secrete salt and fluid, but also provide lactate as an essential nutrient (Jutte *et al.*, 1982), and phagocytose large portions of the cytoplasm of spermatids. The blood–testis barrier requires that Sertoli cells transport or synthesize many essential nutrients, e.g. transferrin-bound iron.

Testicular degeneration in *Clcn2−/−* mice begins at ~2 weeks of age, concomitant with the establishment of the blood–testis barrier (Waites and Gladwell, 1982; Byers *et al.*, 1991). The lack of lumina in seminiferous tubules suggests a defect in transepithelial transport by Sertoli cells, which express ClC-2 at their cell surface and whose morphology is abnormal in −/− mice. While this could explain the degeneration of germ cells in the adluminal compartment, it can not directly explain the loss of spermatogonia at the *cis* side of the barrier. However, ClC-2 is also expressed in membrane patches that face the germ cells at the *cis* side, and could therefore influence the ionic homeostasis in these clefts as well. Sertoli cells produce lactate as a nutrient for germ cells. The transport of lactate across membranes is mediated by H+–lactate cotransporters (Halestrap and Price, 1999), creating the need for an efficient pH regulation both in the cytoplasm and in the narrow extracellular clefts between Sertoli and germ cells. ClC-2 opens in response to extracellular acidification (Jordt and Jentsch, 1997). This activation might be needed to regulate $HCO_3^−$ transport by creating a Cl−-recycling pathway for $HCO_3^−$/Cl− exchangers.

Male infertility has been observed with mutations in some other ion channels or ion transporters, but was not associated with a total loss of germ cells. A mutation in the GIRK2 K+ channel causes male infertility (and a cerebellar phenotype) in the *weaver* mouse (Harrison and Roffler-Tarlov, 1998). However, this is due to an altered ion selectivity of the mutated channel, and mice deleted for GIRK2 are fertile (Signorini *et al.*, 1997). Male patients with mutations in CFTR, the Cl− channel defective in cystic fibrosis, are also infertile. However, infertility is due to defects in the epididymis and the vas deferens (Wong, 1998) and male CFTR−/− mice are fertile (Snouwaert *et al.*, 1992). Recently, defective spermatogenesis was reported for a Na+–K+–2Cl− cotransporter (NKCC1) knock-out mouse model (Pace *et al.*, 2000), which displays several other organ abnormalities in addition to infertility. It was speculated that NKCC1 led to a defect in the production of tubular fluid. In contrast to the present model, the loss of germ cells was not complete.

Additionally, we observed a severe retinal degeneration that eventually led to a complete loss of photoreceptor cells. Interestingly, it began at about the same time as the testicular degeneration, and its onset coincided with the formation of the blood–organ barrier in both tissues. In the eye, this barrier is formed by the RPE (Tserentsoodol *et al.*, 1998). In an interesting analogy to Sertoli cell–germ cell interactions, the RPE has close spatial and functional relationships with photoreceptors. Similarly to Sertoli cells, the RPE transports fluid and lactate (Zeuthen *et al.*, 1996; Philp *et al.*, 1998), is involved in phagocytosis of outer segments that are shed from photoreceptors, and synthesizes and transports metabolites (e.g. retinoids). It is therefore tempting to speculate that ClC-2 is similarly involved in the ionic homeostasis of the narrow subretinal space that is formed between the RPE and photoreceptors.

Similar to the situation in seminiferous tubules, the lactate transport poses problems for the regulation of pH (Kenyon *et al.*, 1997). ClC-2 may play an important role in the regulation of pH in this compartment, or in the fluid transport across the RPE, which is important to prevent retinal detachment. Because ClC-2 is not only expressed in the neuronal retina, but also in the RPE (Figure 7B and C and Enz *et al.*, 1999), we tested directly in Ussing chamber experiments whether the disruption of ClC-2 affects the electrical current across the RPE. Ideally, these experiments should be performed at a time when possible secondary effects of the retinal degeneration on the RPE can be excluded. However, given the early onset of the degeneration, the small size of mice and the post-natal development of tight junctions in the RPE, this turned out to be impossible. We therefore performed our experiments with P36 mice, which have marked, but not yet complete retinal degeneration. There was a drastic decrease in transepithelial voltage, resistance and current, demonstrating that the function of the RPE is severely compromised. This is compatible with the notion that photoreceptors degenerate as a consequence of an altered microenvironment created by the RPE.

In summary, the knock-out of the broadly expressed Cl⁻ channel ClC-2 did not support several previous hypotheses about its physiological roles. Rather, it provided the unexpected insight that it is important for the function of two of the most highly differentiated tissues: the seminiferous tubule of the testis and the photoreceptors of the retina. It seems that the function of ClC-2 is most critical for cells that depend on a closely associated and actively transporting epithelium for their function and survival. Future studies involving the disruption of both ClC-2 and CFTR, the epithelial Cl⁻ channel mutated in cystic fibrosis, will reveal whether it also plays a role in those epithelia affected by that important disease.

Materials and methods

Generation of ClC-2 knock-out mice

A clone isolated from a 129/SvJ mouse genomic λ library (Stratagene) was used to construct a targeting vector with a PGK-neo-bpA (neo) cassette as a positive and the diphtheria toxin α subunit cassette (dta) as a negative selection marker. The neo cassette replaced 931 bp encoding part of exon 4 and exons 5–8 of ClC-2. The linearized vector was electroporated into R1 ES cells, and G418-resistant clones were screened by Southern blotting using a 5′ 600 bp *Not*I–*Hin*dIII fragment outside the targeting vector. Digestion of genomic DNA with *Eco*RI resulted in 12 kb (WT) versus 8 kb (mutant allele), and with *Nhe*I in 4.1 kb (WT) versus 3.5 kb (mutant allele). A correctly targeted ES cell clone was injected into C57BL/6 blastocysts to generate chimeras that were backcrossed with strain C57BL/6. Heterozygous offspring were crossed to yield homozygous mutant animals. The present studies were performed with the F_2 and F_3 generations of ClC-2 knock-out mice. We also obtained a second independent $Clcn2^{-/-}$ line with a slightly different construct and RW4 ES cells. Its phenotype was indistinguishable from that described here.

In situ hybridization

Antisense RNA probes labeled with [α-^{35}S]UTP (1000–1500 Ci/mmol; NEN) were transcribed with T7 polymerase from linearized *Clcn2* cDNA clones (nucleotides 74–903 and 845–1405) according to the instructions of the manufacturer (Ambion) and purified on a Sephadex G50 spin column (Roche). Serial 10 μm sections were cut in a cryostat, fixed in 4% paraformaldehyde in phosphate-buffered saline (PBS), acetylated, dehydrated and hybridized. Sections were dehydrated and exposed to high-resolution X-ray films (Kodak Biomax). The slides were then dipped into Kodak NTB-2 nuclear track emulsion, developed after 3–6 weeks in Kodak Dektol and stained with Giemsa (Sigma). Specificity of the signals was verified by comparing two independent probes and by using sense probes.

Northern analysis

RNA was prepared from testes with the Trizol reagent (Life Technologies) according to the manufacturer's instructions. Each lane was loaded with 10 μg of total RNA. Probes were cloned by RT–PCR from mouse testes RNA with the following lengths: protamine, 285 bp; cyclin A1, 765 bp; proacrosin binding protein, 330 bp.

Histology and immunocytochemistry

For semi-thin section histology and electron microscopy, testes were pre-fixed in 3.5% glutaraldehyde in 0.05 M sodium phosphate buffer pH 7.1–7.4, post-fixed in 1% OsO₄ and finally embedded in Epon 812. Semi-thin sections were stained with toluidine blue and pyronine G. For immunohistochemistry, paraffin sections from material immersed in Bouin's fixative were used. Antibodies were generated in rabbits against a C-terminal ClC-2 peptide (HGLPREGTPSDSDDKCQ) *m*-maleimido-benzoyl-*N*-hydroxysuccinimide ester coupled to bovine serum albumin. The affinity-purified serum recognized a band of the expected size in cells transfected with ClC-2 that gave only a faint signal in non-transfected cells. In protein lysates of testes obtained from $Clcn2^{-/-}$ animals, no band was detected (Figure 1D). The antibody was used in immunocyto-chemistry at a 1:50 dilution. A commercial ClC-2 antibody (Alomone) did not prove useful.

Patch–clamp experiments

Leydig cells were purified from +/+ and –/– mice on Percoll gradients as described (Schumacher *et al.*, 1978). Briefly, testes were removed and decapsulated; crude cell suspension was layered on top of the gradient and centrifuged for 20 min at 800 *g*. Four visible bands of testicular cells were obtained. Highly purified Leydig cells were found in the third band from the top. The purity of Leydig cells was determined as described (Steinberger *et al.*, 1966). Sertoli cells were purified by trypsin digestion of tubuli at 30°C (Gorczynska *et al.*, 1994). After 1–2 days in MEM culture medium, currents were examined by whole-cell patch–clamping using an Axopatch 200A amplifier and pCLAMP software. The cells were bathed in 146 mM CsCl, 2 mM CaCl₂, 10 mM HEPES pH 7.4, and the internal pipette solution was 146 mM CsCl, 10 mM HEPES, 5 mM EGTA pH 7.4.

Ussing chamber experiments

Mice were killed by cervical dislocation, the eyes removed and immediately immersed in Ringer's solution, perforated with a fine hypodermic needle, and cut open along the ora serrata. The neural retina was carefully detached from the underlying RPE, dissecting the optic nerve fibers as completely as possible. Resulting pieces of RPE on its scleral support were attached to the insert of a custom-made Ussing chamber allowing rapid solution exchange and fixed with a bronze spring. The opening area was 1 mm². During the experiment, solution was switched from phosphate-buffered Ringer's solution to HCO₃⁻-buffered Ringer's solution, which increased the transepithelial voltage (V_{te}), but as there was a rapid rundown of both V_{te} and R_{te}, only initial parameters were included in the results. V_{te} was measured by a custom-made electrometer. Resistance was calculated by V_{te} deflections induced by current injection (0.1 μA). I'_{sc} was calculated according to Ohm's law.

Gastric acidification, serum hormones and steroidogenesis in Leydig cells

Fifteen minutes after s.c. injection of histamine (2 μg/g body weight) or PBS (as solvent control), gastric acidification was measured as described (Schultheis *et al.*, 1998). Serum FSH, LH, testosterone and progesterone were determined by radioimmunoassays (RIA), and progesterone by ELISA. The capacity of testosterone production and release by Leydig cells was compared *in vitro* between WT, $Clcn2^{+/-}$ and $Clcn2^{-/-}$ males. Purified Leydig cells (5–10 × 10⁴ cells) were incubated in 500 μl of medium for 3 h at 36°C and testosterone release was stimulated with either hCG or 8-Br-cAMP at various concentrations. Testosterone released into the medium supernatant was assayed by RIA.

References

Blaisdell,C.J., Edmonds,R.D., Wang,X.T., Guggino,S. and Zeitlin,P.L. (2000) pH-regulated chloride secretion in fetal lung epithelia. *Am. J. Physiol. Lung Cell Mol. Physiol.*, **278**, L1248–L1255.

Byers,S., Graham,R., Dai,H.N. and Hoxter,B. (1991) Development of Sertoli cell junctional specializations and the distribution of the tight-junction-associated protein ZO-1 in the mouse testis. *Am. J. Anat.*, **191**, 35–47.

Cherubini,E., Gaiarsa,J.L. and Ben-Ari,Y. (1991) GABA: an excitatory transmitter in early postnatal life. *Trends Neurosci.*, **14**, 515–519.

Choi,M.S. and Cooke,B.A. (1990) Evidence for two independent pathways in the stimulation of steroidogenesis by luteinizing hormone involving chloride channels and cyclic AMP. *FEBS Lett.*, **261**, 402–404.

Enders,G.C. and May,J.J.,II (1994) Developmentally regulated expression of a mouse germ cell nuclear antigen examined from embryonic day 11 to adult in male and female mice. *Dev. Biol.*, **163**, 331–340.

Enz,R., Ross,B.J. and Cutting,G.R. (1999) Expression of the voltage-gated chloride channel ClC-2 in rod bipolar cells of the rat retina. *J. Neurosci.*, **19**, 9841–9847.

Fahlke,C., Yu,H.T., Beck,C.L., Rhodes,T.H. and George,A.L.,Jr (1997) Pore-forming segments in voltage-gated chloride channels. *Nature*, **390**, 529–532.

Furukawa,T., Ogura,T., Katayama,Y. and Hiraoka,M. (1998) Characteristics of rabbit ClC-2 current expressed in *Xenopus* oocytes and its contribution to volume regulation. *Am. J. Physiol.*, **274**, C500–C512.

Gorczynska,E., Spaliviero,J. and Handelsman,D.J. (1994) The relationship between 3′,5′-cyclic adenosine monophosphate and calcium in mediating follicle-stimulating hormone signal transduction in Sertoli cells. *Endocrinology*, **134**, 293–300.

Gründer,S., Thiemann,A., Pusch,M. and Jentsch,T.J. (1992) Regions involved in the opening of ClC-2 chloride channel by voltage and cell volume. *Nature*, **360**, 759–762.

Günther,W., Lüchow,A., Cluzeaud,F., Vandewalle,A. and Jentsch,T.J. (1998) ClC-5, the chloride channel mutated in Dent's disease, colocalizes with the proton pump in endocytotically active kidney cells. *Proc. Natl Acad. Sci. USA*, **95**, 8075–8080.

Halestrap,A.P. and Price,N.T. (1999) The proton-linked monocarboxylate transporter (MCT) family: structure, function and regulation. *Biochem. J.*, **343**, 281–299.

Harrison,S.M. and Roffler-Tarlov,S.K. (1998) Cell death during development of testis and cerebellum in the mutant mouse *weaver*. *Dev. Biol.*, **195**, 174–186.

Huber,S., Schroppel,B., Kretzler,M., Schlöndorff,D. and Horster,M. (1998) Single cell RT–PCR analysis of ClC-2 mRNA expression in ureteric bud tip. *Am. J. Physiol.*, **274**, F951–F957.

Jackson,P.S. and Strange,K. (1995) Single-channel properties of a volume-sensitive anion conductance. Current activation occurs by abrupt switching of closed channels to an open state. *J. Gen. Physiol.*, **105**, 643–660.

Jentsch,T.J., Friedrich,T., Schriever,A. and Yamada,H. (1999) The CLC chloride channel family. *Pflugers Arch.*, **437**, 783–795.

Jordt,S.E. and Jentsch,T.J. (1997) Molecular dissection of gating in the ClC-2 chloride channel. *EMBO J.*, **16**, 1582–1592.

Jutte,N.H., Jansen,R., Grootegoed,J.A., Rommerts,F.F., Clausen,O.P. and van der Molen,H.J. (1982) Regulation of survival of rat pachytene spermatocytes by lactate supply from Sertoli cells. *J. Reprod. Fertil.*, **65**, 431–438.

Kenyon,E., Maminishkis,A., Joseph,D.P. and Miller,S.S. (1997) Apical and basolateral membrane mechanisms that regulate pHi in bovine retinal pigment epithelium. *Am. J. Physiol.*, **273**, C456–C472.

Koch,M.C. *et al.* (1992) The skeletal muscle chloride channel in dominant and recessive human myotonia. *Science*, **257**, 797–800.

Kornak,U., Kasper,D., Bösl,M.R., Kaiser,E., Schweizer,M., Schulz,A.,

Friedrich,W., Delling,G. and Jentsch,T.J. (2001) Loss of the ClC-7 chloride channel leads to osteopetrosis in mice and man. *Cell*, **104**, 205–215.

la Cour,M., Lund-Andersen,H. and Zeuthen,T. (1986) Potassium transport of the frog retinal pigment epithelium: autoregulation of potassium activity in the subretinal space. *J. Physiol. (Lond.)*, **375**, 461–479.

Lee,K., Haugen,H.S., Clegg,C.H. and Braun,R.E. (1995) Premature translation of protamine 1 mRNA causes precocious nuclear condensation and arrests spermatid differentiation in mice. *Proc. Natl Acad. Sci. USA*, **92**, 12451–12455.

Lloyd,S.E. *et al.* (1996) A common molecular basis for three inherited kidney stone diseases. *Nature*, **379**, 445–449.

Ludewig,U., Pusch,M. and Jentsch,T.J. (1996) Two physically distinct pores in the dimeric ClC-0 chloride channel. *Nature*, **383**, 340–343.

Malinowska,D.H., Kupert,E.Y., Bahinski,A., Sherry,A.M. and Cuppoletti,J. (1995) Cloning, functional expression and characterization of a PKA-activated gastric Cl⁻ channel. *Am. J. Physiol.*, **268**, C191–C200.

Matsumura,Y. *et al.* (1999) Overt nephrogenic diabetes insipidus in mice lacking the CLC-K1 chloride channel. *Nature Genet.*, **21**, 95–98.

Murray,C.B., Morales,M.M., Flotte,T.R., McGrath-Morrow,S.A., Guggino,W.B. and Zeitlin,P.L. (1995) ClC-2: a developmentally dependent chloride channel expressed in the fetal lung and downregulated after birth. *Am. J. Respir. Cell Mol. Biol.*, **12**, 597–604.

Nantel,F., Monaco,L., Foulkes,N.S., Masquilier,D., LeMeur,M., Henriksen,K., Dierich,A., Parvinen,M. and Sassone-Corsi,P. (1996) Spermiogenesis deficiency and germ-cell apoptosis in CREM-mutant mice. *Nature*, **380**, 159–162.

Noulin,J.F. and Joffre,M. (1993) Characterization and cyclic AMP-dependence of a hyperpolarization-activated chloride conductance in Leydig cells from mature rat testis. *J. Membr. Biol.*, **133**, 1–15.

Noulin,J.F., Fayolle-Julien,E., Desaphy,J.F., Poindessault,J.P. and Joffre,M. (1996) Swelling and cAMP on hyperpolarization-activated Cl⁻ conductance in rat Leydig cells. *Am. J. Physiol.*, **271**, C74–C84.

Pace,A.J., Lee,E., Athirakul,K., Coffman,T.M., O'Brien,D.A. and Koller,B.H. (2000) Failure of spermatogenesis in mouse lines deficient in the Na⁺–K⁺–2Cl⁻ cotransporter. *J. Clin. Invest.*, **105**, 441–450.

Philp,N.J., Yoon,H. and Grollman,E.F. (1998) Monocarboxylate transporter MCT1 is located in the apical membrane and MCT3 in the basal membrane of rat RPE. *Am. J. Physiol.*, **274**, R1824–R1828.

Piwon,N., Günther,W., Schwake,M., Bösl,M.R. and Jentsch,T.J. (2000) ClC-5 Cl⁻-channel disruption impairs endocytosis in a mouse model for Dent's disease. *Nature*, **408**, 369–373.

Prichard,J.W., Gallagher,B.B. and Glaser,G.H. (1969) Experimental seizure-threshold testing with fluorthyl. *J. Pharmacol. Exp. Ther.*, **166**, 170–178.

Protopopov,A.I. *et al.* (1996) Human chromosome 3: high-resolution fluorescence *in situ* hybridization mapping of 40 unique *Not*I linking clones homologous to genes and cDNAs. *Chromosome Res.*, **4**, 443–447.

Rivera,C., Voipio,J., Payne,J.A., Ruusuvuori,E., Lahtinen,H., Lamsa,K., Pirvola,U., Saarma,M. and Kaila,K. (1999) The K⁺/Cl⁻ co-transporter KCC2 renders GABA hyperpolarizing during neuronal maturation. *Nature*, **397**, 251–255.

Sander,T. *et al.* (2000) Genome search for susceptibility loci of common idiopathic generalised epilepsies. *Hum. Mol. Genet.*, **9**, 1465–1472.

Schultheis,P.J. *et al.* (1998) Targeted disruption of the murine Na⁺/H⁺ exchanger isoform 2 gene causes reduced viability of gastric parietal cells and loss of net acid secretion. *J. Clin. Invest.*, **101**, 1243–1253.

Schumacher,M., Schafer,G., Holstein,A.F. and Hilz,H. (1978) Rapid isolation of mouse Leydig cells by centrifugation in Percoll density gradients with complete retention of morphological and biochemical integrity. *FEBS Lett.*, **91**, 333–338.

Schwiebert,E.M., Cid-Soto,L.P., Stafford,D., Carter,M., Blaisdell,C.J., Zeitlin,P.L., Guggino,W.B. and Cutting,G.R. (1998) Analysis of ClC-2 channels as an alternative pathway for chloride conduction in cystic fibrosis airway cells. *Proc. Natl Acad. Sci. USA*, **95**, 3879–3884.

Signorini,S., Liao,Y.J., Duncan,S.A., Jan,L.Y. and Stoffel,M. (1997) Normal cerebellar development but susceptibility to seizures in mice lacking G protein-coupled, inwardly rectifying K⁺ channel GIRK2. *Proc. Natl Acad. Sci. USA*, **94**, 923–927.

Simon,D.B. *et al.* (1997) Mutations in the chloride channel gene, *CLCNKB*, cause Bartter's syndrome type III. *Nature Genet.*, **17**, 171–178.

Smith,R.L., Clayton,G.H., Wilcox,C.L., Escudero,K.W. and Staley,K.J.

(1995) Differential expression of an inwardly rectifying chloride conductance in rat brain neurons: a potential mechanism for cell-specific modulation of postsynaptic inhibition. *J. Neurosci.*, **15**, 4057–4067.

Snouwaert,J.N., Brigman,K.K., Latour,A.M., Malouf,N.N., Boucher,R.C., Smithies,O. and Koller,B.H. (1992) An animal model for cystic fibrosis made by gene targeting. *Science*, **257**, 1083–1088.

Solc,C.K. and Wine,J.J. (1991) Swelling-induced and depolarization-induced C1⁻ channels in normal and cystic fibrosis epithelial cells. *Am. J. Physiol.*, **261**, C658–C674.

Staley,K. (1994) The role of an inwardly rectifying chloride conductance in postsynaptic inhibition. *J. Neurophysiol.*, **72**, 273–284.

Staley,K., Smith,R., Schaack,J., Wilcox,C. and Jentsch,T.J. (1996) Alteration of GABA$_A$ receptor function following gene transfer of the CLC-2 chloride channel. *Neuron*, **17**, 543–551.

Steinberger,E., Steinberger,A. and Vilar,O. (1966) Cytochemical study of δ-5-3-β-hydroxysteroid dehydrogenase in testicular cells grown *in vitro*. *Endocrinology*, **79**, 406–410.

Steinmeyer,K., Lorenz,C., Pusch,M., Koch,M.C. and Jentsch,T.J. (1994) Multimeric structure of ClC-1 chloride channel revealed by mutations in dominant myotonia congenita (Thomsen). *EMBO J.*, **13**, 737–743.

Stobrawa,S.M. *et al.* (2001) Disruption of ClC-3, a chloride channel expressed on synaptic vesicles, leads to a loss of the hippocampus. *Neuron*, **29**, 185–196.

Strange,K., Emma,F. and Jackson,P.S. (1996) Cellular and molecular physiology of volume-sensitive anion channels. *Am. J. Physiol.*, **270**, C711–C730.

Sweeney,C., Murphy,M., Kubelka,M., Ravnik,S.E., Hawkins,C.F., Wolgemuth,D.J. and Carrington,M. (1996) A distinct cyclin A is expressed in germ cells in the mouse. *Development*, **122**, 53–64.

Thiemann,A., Gründer,S., Pusch,M. and Jentsch,T.J. (1992) A chloride channel widely expressed in epithelial and non-epithelial cells. *Nature*, **356**, 57–60.

Tserentsoodol,N., Shin,B.C., Suzuki,T. and Takata,K. (1998) Colocalization of tight junction proteins, occludin and ZO-1 and glucose transporter GLUT1 in cells of the blood–ocular barrier in the mouse eye. *Histochem. Cell Biol.*, **110**, 543–551.

Waites,G.M. and Gladwell,R.T. (1982) Physiological significance of fluid secretion in the testis and blood–testis barrier. *Physiol. Rev.*, **62**, 624–671.

Wong,P.Y. (1998) CFTR gene and male fertility. *Mol. Hum. Reprod.*, **4**, 107–110.

Worrell,R.T., Butt,A.G., Cliff,W.H. and Frizzell,R.A. (1989) A volume-sensitive chloride conductance in human colonic cell line T84. *Am. J. Physiol.*, **256**, C1111–C1119.

Xiong,H., Li,C., Garami,E., Wang,Y., Ramjeesingh,M., Galley,K. and Bear,C.E. (1999) ClC-2 activation modulates regulatory volume decrease. *J. Membr. Biol.*, **167**, 215–221.

Zeuthen,T., Hamann,S. and la Cour,M. (1996) Cotransport of H⁺, lactate and H$_2$O by membrane proteins in retinal pigment epithelium of bullfrog. *J. Physiol. (Lond.)*, **497**, 3–17.